RSC Advances

PAPER

View Article Online
View Journal | View Issue

Cite this: *RSC Adv.*, 2024, **14**, 20553

Influence of halogen–halogen interactions in the self-assembly of pillar[5]arene-based supramolecular polymers†

Mickey Vinodh, Anwar A. Alshammari and Talal F. Al-Azemi *

Halogen–halogen interactions play a pivotal role in the formation and stability of supramolecular assemblies. Herein, we investigate the assembly dynamics and dissociation pathways of linear supramolecular polymers based on pillar[5]arene-mediated by guest halogen–halogen interactions (C–X × X–C) in both the solution and solid states. The structure of the solid-state supramolecular assembly was determined by single-crystal X-ray diffraction analysis. The binding affinities of four different 1,4-dihalobutane guests with pillar[5]arene were investigated by ^{1}H NMR spectroscopic titration and isothermal titration calorimetry (ITC). The formation of the halogen-bonded linear supramolecular polymer in solution was demonstrated using diffusion-ordered spectroscopy (DOSY) and ITC. Our findings highlight the dependence of the dissociation process on halogen nature within the encapsulated guest, revealing that the process is entropically driven ($T\Delta S$ = 27.12 kJ mol^{-1}) and enthalpically disfavored (ΔH = 9.99 kJ mol^{-1}). Moreover, the disassembly of supramolecular polymers promoted by N-containing compounds was investigated using ^{1}H NMR spectroscopy and ITC, revealing that the process is driven both enthalpically (ΔH = −2.64 kJ mol^{-1}) and entropically ($T\Delta S$ = 15.70 kJ mol^{-1}). Notably, the data suggest the formation of N···I bonding interactions at both ends of the inclusion guest, elucidating the intricate interplay of halogen interactions and host–guest chemistry in supramolecular polymer systems.

Received 22nd May 2024
Accepted 24th June 2024

DOI: 10.1039/d4ra03769c

rsc.li/rsc-advances

Introduction

Supramolecular chemistry explores interactions beyond traditional covalent bonds, such as hydrogen bonding, host–guest recognition, and π–π interactions.[1–16] Of particular interest is molecular self-assembly, a captivating phenomenon in chemistry and materials science.[17–24] This process occurs when molecules arrange themselves spontaneously into precise structures or patterns without external guidance or intervention. Central to this field are supramolecular polymers, which emerge from dynamic non-covalent interactions between small molecules, oligomers, or polymers. Characterized by their reversible nature and responsiveness to external stimuli, these polymers display unique properties.

Macrocycle host molecules play important roles in supramolecular chemistry, these include crown ethers,[25–27] calixarenes,[28] cucurbiturils,[29] and cyclodextrins.[30–32] Among these, pillararenes and their structurally similar scaffolds have attracted considerable attention owing to their interesting conformational, physicochemical, and host–guest properties.[33–35] The different properties and architectures of macrocycles afford them the versatile capability to bind with different guest molecules. Notably, pillar[*n*]arenes represent a novel class of macrocyclic hosts characterized by their electron-rich cavities and finely adjustable rims.[36] Their straightforward synthesis and remarkable properties render them as excellent candidates for constructing advance materials. Pillar[*n*]arene-based supramolecular polymers have applications in various fields like fluorescence sensing, substance adsorption and separation, catalysis, light-harvesting systems, artificial nanochannels, and drug delivery.[36]

Halogen bonding has emerged as an effective tool for assembling supramolecular polymers in both solid and solution states.[37–42] Heavy halogens, in particular, exhibit electrophilic characteristics due to the anisotropic distribution of electrostatic potential around their atomic centers, enabling interactions with electron-pair-donating heteroatoms (O, N, and S) or anions. Consequently, they have been widely utilized in the assembly of diverse supramolecular systems. The most frequently used halogen bond donor is iodine, especially in haloarenes and haloalkynes, owing to its ability to form strong and accessible halogen bonds. For instance, (N···I) halogen-bonded linear supramolecular polymers based on pillar[5]arenes have been developed involving either a N-containing guest

Chemistry Department, Kuwait University, P.O. Box 5969, Safat 13060, Kuwait. E-mail: t.alazemi@ku.edu.kw; Fax: +965-2481-6482; Tel: +965-2498-5631

† Electronic supplementary information (ESI) available. CCDC 1969977, 2343042–2343044. For ESI and crystallographic data in CIF or other electronic format see DOI: https://doi.org/10.1039/d4ra03769c

or one built into the macrocycle, linked together by diiodo-compounds.[36–39] In contrast, halogen–halogen interactions are a particularly interesting subclass of halogen bonds and serve as essential design elements in crystal engineering.[43–45] In this context, halogen bonds, particularly those based on halogen–halogen interactions, stand as essential design elements. However, their weakness in the solution state poses challenges for characterization or detection.[40–42]

Recently, we reported macrocycle-based supramolecular polymer assemblies mediated by bromine–bromine guest interactions in solution.[46,47] Building upon this, the present work investigates the influence halogen nature in 1,4-halobutane guests on the mediation of pillar[5]arene-based supramolecular polymer assemblies *via* halogen–halogen bond interactions. Various techniques, such as X-ray single-crystal diffraction, ^{1}H NMR spectroscopy, diffusion-order spectroscopy (DOSY), and isothermal titration calorimetry (ITC) dilution experiments have been utilized to scrutinize supramolecular assemblies in both solution and solid phases. Moreover, the supramolecular polymer disassembly process influenced by external stimuli was explored using nitrogen-containing compounds.

Results and discussion

Crystal structure determination

In our ongoing efforts to investigate supramolecular polymer assembly facilitated by guest halogen–halogen interactions,[46,47] we conducted a comparative assessment of four 1,4-dihalobutane guests-namely 1,4-diflourobutane (**DFB**), 1,4-dichlorobutane (**DCB**), 1,4-dibromobutane (**DBB**) and 1,4-diiodobutane (**DIB**) with permethylated pillar[5]arene **DMP5** host for their ability to promote self-assemble supramolecular polymers. While the complexation of 1,4-dihalobutanes with dialkoxypillar[5]arenes has been reported using ^{1}H NMR spectroscopic titration methods,[48,49] their ability to promote supramolecular assembly has not been evaluated. The incorporation of ethoxy, butoxy, and octoxy substituents in both rims of the pillar[5]arene cavities prevented halogen–halogen interactions in the resulting inclusion crystal structures with **DFB**, **DCB** and **DIB** guests, respectively.[48] Similarly, the crystal structure analysis of a large A1/A2-dibromohexyl substituent copillar[5]arene with **DBB** revealed no guest-driven supramolecular polymer assembly.[49] Nevertheless, the complexation of permethylated pillar[5]arenes (**DMP5**) with **DFB**, **DCB** and **DIB** guests in solution, along with their corresponding inclusion crystal structures have not been reported. To address this gasp, suitable crystals of **DMP5** with **DXB** (X = F, Cl, Br, or I) were grown using the slow evaporation/diffusion method with dichloromethane. Subsequent crystal structure analysis of the obtained inclusion complexes [**DPM5** ⊃ **DXB**] revealed that all 1,4-dihaloalkanes were stabilized by C–H···π or C–H···O interactions inside the pillar[5]arene cavity.

Previously, we successfully demonstrated the ability of the host–guest inclusion complex of **DMP5** and **DBB** to facilitate the self-assembly of linear supramolecular polymers in both solid and solution phases through guest halogen–halogen interactions (C–Br···Br–C).[46] Inspection of the crystal structures of the inclusion complexes of [**DMP5** ⊃ **DCB**] and [**DMP5** ⊃ **DIB**] revealed similar behavior in the solid state, with variations attributed to the nature of the halogen atoms within the guest molecule (Fig. 1). The linear supramolecular assembly driven by the interactions between the iodine atom of one **DIB** molecule located inside the **DMP5** cavity and that inside the adjacent inclusion complex, is significantly intensified by (I···I) interactions compare to its corresponding (Br···Br) counterpart. This is evidenced by the calculated separation of 3.508 Å for I···I which is approximately 16.8% shorter than the sum of the respective van der Waals atomic radii (4.2 Å), whereas the Br···Br separation of 3.398 Å is shorter by approximately 8.2% of the sum of the respective van der Waals atomic radii (3.7 Å). In [**DPM5** ⊃ **DCB**], the Cl···Cl distance of adjacent **DCB** molecules in the linear network is 3.59 Å similar to the sum of their respective van der Waals atomic radii (3.6 Å). All halogen–halogen interaction (X···X) adopt a *trans* type I ($\theta_1 \approx \theta_2$) configuration based on the C–X···X angles θ_1 and θ_2. Interestingly, the [**DPM5** ⊃ **DFB**] inclusion complex does not exhibit linear propagation in the crystal network; instead, two adjacent inclusion complexes align in an edge-to-face manner (Fig. 1).

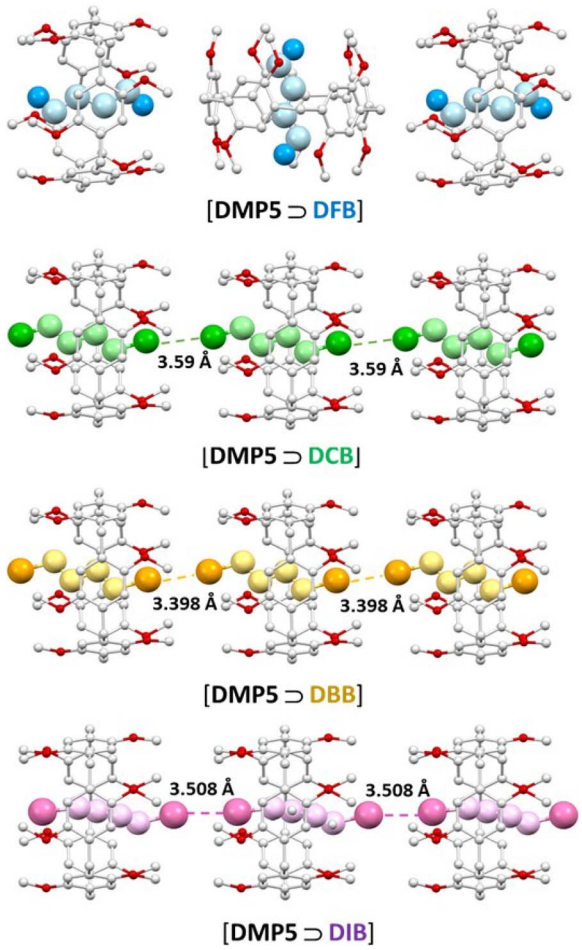

Fig. 1 Crystal structures of the inclusion complexes obtained from the co-crystallization of premethylated pillar[5]arene (DMP5) with four different 1,4-dihalobutanes. (blue, F; green, Cl; purple, I; hydrogen atoms are omitted for clarity).

Hirshfeld surface analysis

The visualization of intermolecular interactions in the inclusion crystals was facilitated by Hirshfeld surface analysis, a powerful tool for gaining additional insights into crystal structures.[50–52] This analysis comprises two main features: three-dimensional (3D) d_{norm} surface images and two-dimensional (2D) fingerprint plots. The 3D d_{norm} surface allows for the analysis and visualization of intermolecular interactions, while the 2D fingerprint plots offer a quantitative summary of the nature and type of intermolecular contacts experienced by the molecules in the crystal. In this study, Hirshfeld surface analysis was conducted using CrystalExplorer 17.1.[53] The 3D d_{norm} surfaces of [**DPM5** ⊃ **DBB**]and [**DPM5** ⊃ **DIB**] exhibit intense red spots at the center of their pillararene cavities, indicative of strong Br···Br and I···I intermolecular contacts shorter than the sum of the relevant van der Waals radii. The white shade at the center of the [**DPM5** ⊃ **DCB**] cavity in Fig. 2 suggests that the Cl···Cl interactions are close to van der Waals contacts, while the blue shade at the center of the [**DPM5** ⊃ **DFB**] cavity confirms the absence of any F···F interactions. From the 2D fingerprint plots, it is observed that the percentage of I···I interactions in the [**DPM5** ⊃ **DIB**] system is higher (1.5%) than the corresponding Br···Br interactions in the [**DPM5** ⊃ **DBB**] (1.3%)**and Cl···Cl interac**tions in the [**DPM5** ⊃ **DCB**] (1.2%). The 2D fingerprint plots reveal that the X···X interactions in the crystal contribute 1.3–5% of the total intermolecular interactions, a significant proportion considering the low number of adjacent halogen atoms in the crystal. In contrast, the inclusion complex [**DPM5** ⊃ **DFB**] showed no F···F interactions in the 2D fingerprint plot (0.0%). Therefore, Hirshfeld surface analysis provides compelling evidence for the role of halogen–halogen interactions in the co-crystal network.

Binding studies

Isothermal titration calorimetry (ITC) has proven to be a valuable tool for studying various reversible non-covalent supramolecular interactions in solution. In this study, quantitative analyses of non-covalent host–guest interactions between **DMP5** and the four 1,4-dihalobutane guests were performed using ITC. The thermodynamic parameters and binding affinities obtained from ITC measurements are summarized in Table 1. Notably, all experimentally obtained binding molar ratios "*n*" are close to one, indicating a 1 : 1 host-to-guest stoichiometric ratio of complexation. However, the association constant (K_a) values are dependent on the halogen nature in the guest molecule. Specifically, the association constant K_a value of the **DFB** guest ($K_a = 1.16 \pm 0.05 \times 10^2$ M^{-1}) was found to be one order of magnitude lower than that of the other 1,4-dihalobutane guests attributed to the weaker dispersion forces exhibited by fluorine upon complexation with **DMP5** host.[48] Moreover, due to its smaller van der Waals volume ($V_{vdw} = 89.9$ Å^3), **DFB** occupied a small fraction of the **DMP5** cavity (*i.e.*, 225 Å^3) leading to weak binding. This is evidenced by the smaller favorable enthalpy change ($\Delta H^\circ = -13.48$ kJ mol^{-1}) compared to the other 1,4-dihalobutanes, indicating weaker van der Waals interactions (Table 1).

The complexation behavior between the host **DMP5** and 1,4-dihalobutanes was further investigated in solution using ^{1}H NMR titration experiments. The chemical shifts (δ) of the phenyl (6.88 ppm) and methoxy (3.74 ppm) protons in ^{1}H NMR spectra of **DMP5** were monitored after the sequential addition of the guests. The appearance of a single set of peaks after addition of the guest indicates fast-exchange complexation on the ^{1}H NMR time scale at 25 °C, consistent with encapsulation behavior reported previously.[46] Association constants for complexation were determined from nonlinear least-squares treatment of the chemical shift changes (δ) of the phenyl proton (Ar–H) at 6.88 ppm for the host *versus* guest concentrations (Fig. S9–S12†). Remarkably, the association constants calculated from the ^{1}H NMR titrations were comparable to the data obtained from ITC measurements (Table 1).

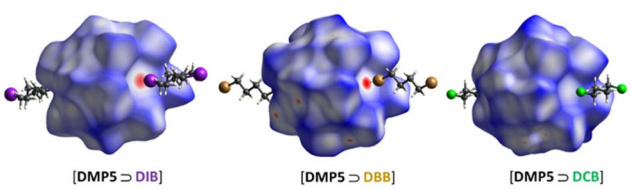

Fig. 2 Hirshfeld surfaces mapped with d_{norm} of the [DMP5 ⊃ DCB], [DMP5 ⊃ DBB] and [DMP5 ⊃ DIB] crystal structures as viewed along the crystallographic *c*-axis directions. The red spots observed at the center of the DMP5 cavity openings indicate strong X···X interactions.

Supramolecular assembly in solution

ITC studies. Supramolecular assembly in solution was investigated using dilution ITC experiments, following our previously reported procedure.[46] This involved sequential injections of a concentrated solution of a supramolecular system into a cell containing a pure solvent. The exchanged heat serves as a measure of the dissociated supramolecular assemblies, reflecting dissociation events. The ITC dilution data for the dissociation of the self-assembled supramolecular polymers into $CHCl_3$ are depicted as a plot of the heat rate (μJ s^{-1}) against time (min), revealing a series of peaks. The area under the endothermic heat peaks provides the enthalpy (ΔH) of dissociation. At sufficiently low concentrations, no further disassembly of the supramolecular assemblies occurred, leaving only the heat of dilution. To underscore the significance of the guest molecule in the supramolecular assembly process, ITC dilution experiments were conducted with the **DMP5** macrocycle at a concentration of 10 mM without the guest molecule. Consistent with previous reports, no significant enthalpy changes were observed.[46] The integrated heat data for a concentrated equimolar solution (10 mM) of the inclusion complexes were fitted to a dissociation model revealing a positive enthalpy of dissociation (ΔH_{diss}). This indicates that the disassembly of the supramolecular complex is driven by an entropically favored process. In contrast, the positive value of enthalpy change (ΔH_{diss}) suggests that disassembly is an enthalpically disfavored process (Table 2) (Fig. 3).

The supramolecular assembly and dissociation equilibrium constants depend on the halogen type of the guest molecule.

Table 1 ITC thermodynamic parameters associated with the complexation between various **DMP5** host and 1,4-dihaloalkane guests[a]

Entry	Guest	$\Delta H^{\circ b}$ (kJ mol^{-1})	$-T\Delta S^{\circ b}$ (kJ mol^{-1})	$K_a{}^b$ (M^{-1})	n^c	$K_a{}^d$ (M^{-1})
1	**DFB**	−13.48	3.65	$1.16 \pm 0.05 \times 10^2$	1.12	$1.48 \pm 0.5 \times 10^2$
2	**DCB**	−24.45	6.39	$1.25 \pm 0.02 \times 10^3$	0.94	$1.92 \pm 0.2 \times 10^3$
3	**DBB**	−24.94	6.40	$1.77 \pm 0.04 \times 10^3$	1.06	$2.16 \pm 0.1 \times 10^3$
4	**DIB**	−25.28	7.09	$1.62 \pm 0.03 \times 10^3$	1.04	$2.73 \pm 0.3 \times 10^3$

[a] Fixed concentration of **DMP5** host (5 mM) and varying guest concentration in chloroform at 25 °C. [b] Calculated from ITC measurements. [c] Experimental binding molar ratios. [d] Calculated by ^{1}H-NMR titration.

The dissociation constant (K_{diss}) for the inclusion complex [**DMP5** ⊃ **DIB**] was determined to be $1.71 \pm 0.03 \times 10^{-4}$ M which is seven and three times slower than [**DMP5** ⊃ **DCB**] and [**DMP5** ⊃ **DBB**], respectively. The strength of the supramolecular assembly driven by I···I interactions was reflected in a higher positive enthalpy change ($\Delta H^\circ = 142.6$ kJ mol^{-1}) relative to assemblies driven by Br···Br ($\Delta H^\circ = 104.8$ kJ mol^{-1}) and Cl···Cl ($\Delta H^\circ = 82.4$ kJ mol^{-1}) interactions. These results are in agreement with reported values of halogen–halogen interaction strength, where larger halogens tend to exhibit larger α-holes (I > Br > Cl > F) and thus form stronger halogen bonds.[54–56] Similar to **DMP5** alone, ITC dilution measurements of a 10 mM equimolar solution of [**DMP5** ⊃ **DFB**] showed no heat exchange related to the dissociation events of the supramolecular assembly, indicating the absence of F–F interactions between adjacent inclusion complexes, as observed in the crystal structure (Fig. 1).

DOSY studies. Diffusion-ordered spectroscopy (DOSY) has been employed to characterize host–guest complexation behaviors and various types of supramolecular assemblies by correlating of ^{1}H NMR signals with the diffusion coefficient (D) in solution. We employed the weight-averaged diffusion coefficients (D) to characterize self-assembled supramolecular polymers mediated by guest Br–Br non-covalent interactions of inclusion complexes based on pillar[5]arene and pagoda[4]arene. According to the Strokes–Einstein equation [$D = k_BT/(6\pi\eta R)$], where T denotes the temperature, k_B is the Boltzmann constant, and η is the dynamic viscosity of the solvent, a change in the diffusion coefficient (D) should be observed in the DOSY spectra because larger aggregates have larger hydrodynamic radii (R), and R is inversely proportional to D.[46,47] The diffusion coefficients (D) obtained from the DOSY measurements of the host–guest systems are summarized in Table 2. The role of the guest molecule in the formation of a self-assembled supramolecular polymer was evidenced by the slower diffusion rate of the inclusion complexes compared to that of **DMP5** without the guest [**DMP5** ⊃ **DFB**] shows similar diffusion coefficient (D) to **DMP5**, indicating that no supramolecular assembly is mediated by halogen–halogen interactions of the guest molecule.

The number-averaged degree of aggregation "supramolecular assembly" can be estimated using the diffusion coefficient obtained from DOSY measurements according to the Stokes–Einstein equation [$N \approx 1/(D/D_{ref})^3$].[47] The number-averaged degree of aggregation "N" is proportional to the reciprocal of the cubic root of the diffusion coefficient, where D and D_{ref} are the diffusion coefficients of [**DMP5** ⊃ **DXB**] and **DMP5** at 5.0 mM (2.1×10^{-9} m^2 s^{-1}), respectively. The number-averaged degrees of supramolecular aggregation were calculated to be 16, 24, and 45 for [**DMP5** ⊃ **DCB**], [**DMP5** ⊃ **DBB**] and [**DMP5** ⊃ **DIB**] respectively. The calculations confirm that the supramolecular polymer assembly was dependent on halogen–halogen interactions between the inclusion complexes in the solution state.

Supramolecular polymer disassembly in solution

Many supramolecular polymer assemblies rely on interactions between electron pair-donating heteroatoms (O, N, and S) or anions and the electrophilic characteristics of heavy halogens. Therefore, many (N···I) halogen-bonded linear supramolecular polymers have been developed, involving a N-containing guest or one integrated into the macrocycle linked together by diiodo-compounds. To explore supramolecular disassembly in solution, N-containing compounds such as 4-dimethylaminopyridine (**DMAP**) pyridine 4-(*tert*-butyl)pyridine, and trimethylamine, were screened for their ability to disassemble the supramolecular polymer based on [**DMP5** ⊃ **DIB**] using ITC titration experiments. These experiments involved the sequential injection of a concentrated solution of N-containing

Table 2 ITC thermodynamic parameters associated with the dilution experiments of various inclusion complexes based on **DMP5** host and 1,4-dihaloalkane guests[a]

Entry	Inclusion complex	$\Delta H^{\circ b}$ (kJ mol^{-1})	$-T\Delta S^{\circ\ b}$ (kJ mol^{-1})	$\Delta S^{\circ b}$ (J mol^{-1})	$K_d{}^b$ (M)	D^c (10^{-10} m^2 S^{-1})
1	[**DMP5** ⊃ **DCB**]	82.4	−68.6	220.2	$1.17 \pm 0.27 \times 10^{-3}$	8.36
2	[**DMP5** ⊃ **DBB**]	104.8	−86.1	288.8	$5.58 \pm 0.16 \times 10^{-4}$	7.27
3	[**DMP5** ⊃ **DIB**]	142.6	−124.7	418.1	$1.71 \pm 0.03 \times 10^{-4}$	5.91

[a] Fixed concentration of the inclusion complex (10 mM) in chloroform at 25 °C. [b] Calculated from ITC measurements. [c] Diffusion coefficient (D) obtained from DOSY measurements.

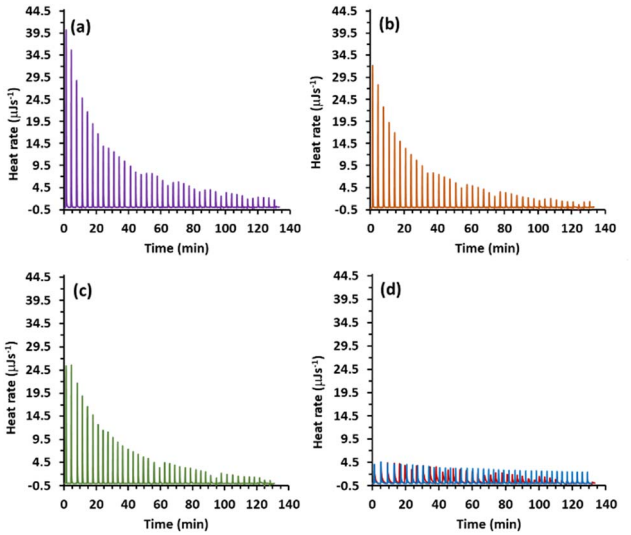

Fig. 3 Raw heat data from ITC dilution experiments for sequential injections in chloroform for the inclusion complexes [DMP5 ⊃ DIB] (a), [DMP5 ⊃ DBB] (b), [DMP5 ⊃ DCB] (c), along with an overly of [DMP5 ⊃ DFB] (blue) with DMP5 alone (red) (d) at 25 °C.

compounds into a cell containing a supramolecular system. The exchanged heat serves as a measure of the dissociated supramolecular assemblies and is characteristic of the dissociation event. It is represented as a plot of heat rate (μJ s^{-1}) against time (min), showing a series of peaks where the area under the endothermic heat peaks provides the enthalpy (ΔH) of dissociation (Fig. S18†). Among the three screened bases, only **DMAP** exhibits significant exchange heat related to the dissociation events of the supramolecular polymer, attributed to the formation of (N···I) halogen bonding (Scheme 1). The binding molar ratios "*n*" calculated from the ITC titration are 2.1, indicating that both iodine atoms in the guest molecule are capped by **DMAP** as illustrated in Scheme 1. The binding association constants (K_a) were determined to be $K_{11} = 6.20 \pm 0.2 \times 10^3$ M^{-1} and $K_{12} = 1.12 \pm 0.3 \times 10^3$ M^{-1}. The supramolecular polymer dissociation process is enthalpically ($\Delta H = -2.64$ kJ mol^{-1}) and entropically driven ($T\Delta S = 15.70$ kJ mol^{-1}), making it a spontaneous process ($\Delta G^\circ = -18.34$ kJ mol^{-1}). The net heat of dissociation promoted by **DMAP5** after integration of the calorimetric traces of [**DMP5** ⊃ **DIB**] as a function of concentration for each injection, was obtained by subtracting the heat of dilution from the reaction heat, and the results are depicted in Fig. 4.

Among the three screened bases, only **DMAP** exhibits significant exchange heat related to the dissociation events of the supramolecular polymer, attributed to the formation of (N···I) halogen bonding (Scheme 1). The binding molar ratios "*n*" calculated from the ITC titration are 2.1, indicating that both iodine atoms in the guest molecule are capped by **DMAP** as illustrated in Scheme 1. The binding association constants (K_a) were determined to be $K_{11} = 6.20 \pm 0.2 \times 10^3$ M^{-1} and $K_{12} = 1.12 \pm 0.3 \times 10^3$ M^{-1}. The supramolecular polymer dissociation process is enthalpically ($\Delta H = -2.64$ kJ mol^{-1}) and entropically driven ($T\Delta S = 15.70$ kJ mol^{-1}), making it a spontaneous process ($\Delta G^\circ = -18.34$ kJ mol^{-1}). The net heat of dissociation promoted by **DMAP5** after integration of the calorimetric traces of [**DMP5** ⊃ **DIB**] as a function of concentration for each injection, was obtained by subtracting the heat of dilution from the reaction heat, and the results are depicted in Fig. 4.

For deeper insights into the host–guest interactions, ^{1}H NMR titration experiments were conducted between 10 mM [**DMP5** ⊃ **DIB**] and various equivalents of **DMAP** in $CDCl_3$ at 298 K (ESI†). Disassembly of the supramolecular polymer was confirmed by the upfield shift of all resonances of the inclusion complex protons. The ^{1}H NMR spectra in $CDCl_3$ of the macrocycle from titration experiments showed only one set of peaks, indicating fast-exchange complexation on the ^{1}H NMR time scale at 25 °C. The stoichiometry of the host–guest complex was determined using the method of continuous variation (Job's plots) between the mole fraction of the base (X_{DMAP}) and the chemical shift changes of aromatic protons (Ph-H) on the pillar[5]arene in ^{1}H NMR, multiplied by the mole fraction (X_{DMAP}). Job's plots of the complexation of [**DMP5** ⊃ **DIB**] with **DMAP** in $CDCl_3$ exhibited maxima at a mole fraction close to 0.33, corresponding to a 1 : 2 stoichiometric ratio of complexation, as depicted in Scheme 1. The methylene protons of the inclusion guest appeared as broad peaks at −0.29 and 1.40 ppm (Fig. 5a). The interaction between the **DMAP** and the inclusion guest is evidenced by the newly formed methylene (–CH_2-I···N) peak at 2.42 ppm after the addition of the base (Fig. 5b). The mode of binding (N···I) was established by comparing the ^{1}H NMR spectra of **DMAP** alone, and [**DMP5** ⊃ **DIB**] with or without the

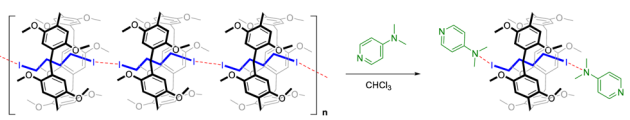

Scheme 1 The dissociation of supramolecular assembly of [DMP5 ⊃ DIB] prompted by 4-dimethylaminopyridine (DMAP).

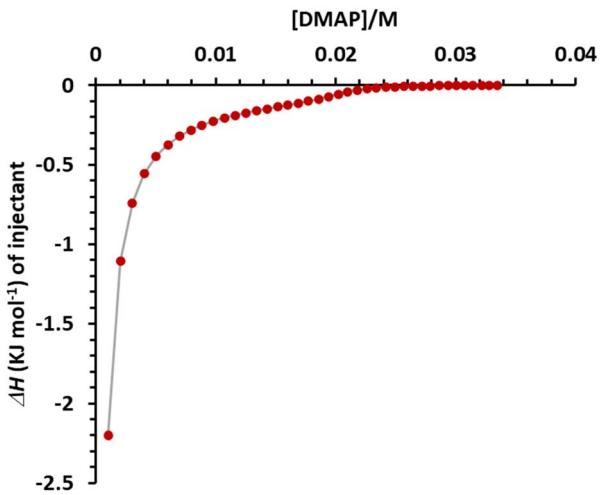

Fig. 4 Net heat of dissociation of 10 mM solutions of [DMP5 ⊃ DIB] promoted by 4-dimethylaminopyridine (DMAP) as a function of concentration (*M*) after subtracting the heat of dilution.

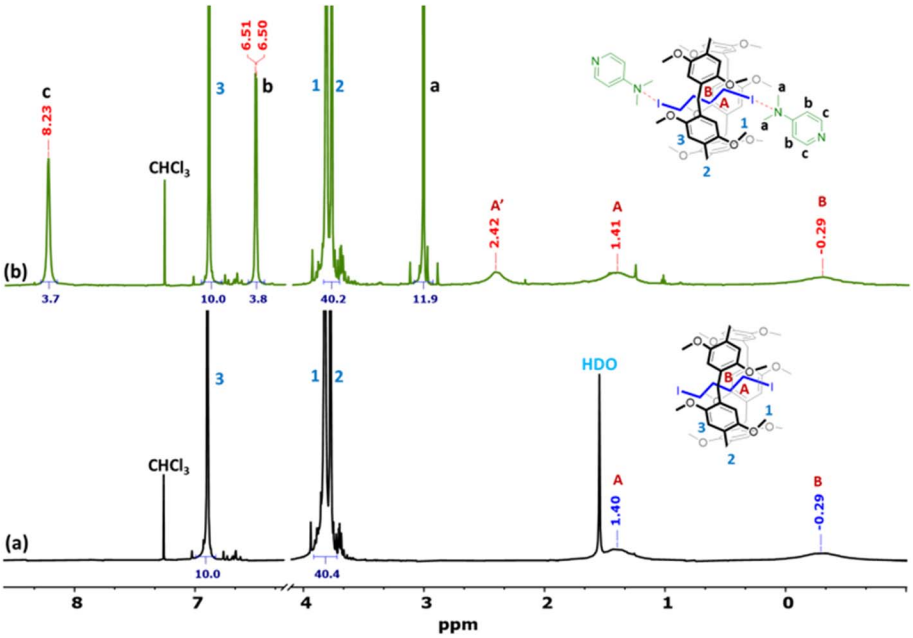

Fig. 5 ^{1}H NMR (600 MHz, chloroform-d, 298 K) spectra of inclusion complex [**DMP5** ⊃ **DIB**] (a), and after addition of 2 equivalents **DMAP** alone (b).

addition two equivalents of the base. The downfield chemical shift from 2.99 to 3.02 ppm observed in the ^{1}H NMR spectrum after the addition of the base suggest that the inclusion guest is capped by the more basic N attached to the dimethyl groups, as expected (Fig. S20†). The association constants for complexation were determined from the nonlinear least-squares treatment of the chemical shift changes (δ) of aromatic protons (Ph-H) at 6.93 ppm for the inclusion complex *versus* **DMAP** concentration (Fig. S21b†). The data fitted well to a 1 : 2 binding isotherm, and the association constants K_a were determined to be $K_{11} = 4.28 \pm 0.2 \times 10^3$ M^{-1} and $K_{12} = 8.17 \pm 0.3 \times 10^2$ M^{-1}. The data obtained from the ^{1}H NMR titrations were in good agreement with those obtained from ITC titration experiments.

Experimental

Materials and methods

NMR spectroscopy was conducted using a Bruker Avance II 600 MHz spectrometer (Germany). Single-crystal data analysis was carried out utilizing R-AXIS RAPID II (Rigaku, Japan) or Bruker X8 prospector (Germany) diffractometers. The data were collected at −123 °C (Oxford Cryosystems, UK). All ITC studies were performed using affinity ITC (TA Instruments, USA) and the data were analyzed using NanoAnalyze software (version 3.10.0). Dimethylformamide (DMF), chloroform, and dichloromethane were distilled prior to use. All other reagents and solvents were of reagent grade and used without further purification. Permethylated pillar[5]arene (**DMP5**) was synthesized following a previously described procedure.[57]

^{1}H NMR titration

A 0.5 mL sample of **DMP5** solution was prepared at a concentration of 5.0 mM in chloroform-d. A guest solution (2 mL) was prepared at a concentration of 0.1 M in chloroform-d. All titration experiments were conducted in NMR tubes at 298 K, and ^{1}H-NMR spectra were recorded upon the successive addition of aliquots of the stock solution of the appropriate guests *via* a microsyringe. The ^{1}H-NMR spectral changes were fitted to a 1 : 1 binding isotherm by nonlinear least-squares treatment using Microsoft Excel to determine the association constant, K_a.[58]

Preparation of single crystals for X-ray diffraction

Single crystals of the inclusion complexes reported in this study were grown using either solvent evaporation or solvent diffusion methods. Crystal data collection was performed using either a Rigaku Rapid II diffractometer with Cu-*K*α radiation or a Bruker X8 prospector diffractometer with Mo-*K*α radiation. The data collected from the Rigaku system were analyzed using the 'Crystalclear' software package. The structures were solved using direct techniques with the crystallographic software program 'CrystalStructure,' and refined using SHELXL-2017/1. Reflection frames from the Bruker system were combined using the Bruker SAINT Software package with the narrow frame method. The structure was then solved and refined using the Bruker SHELXTL Software Package and SHELXL-2017/1. Generation of Single crystals: Slow solvent evaporation of **DMP5** (10 mg) dissolved in a DCM/1,4-dihalobutane solution (9 : 1; v/v, 1 mL) was employed to produce suitable single crystals of inclusion complexes [**DMP5** ⊃ **DFB**] [**DMP5** ⊃ **DCB**], and [**DMP5** ⊃ **DBB**]. To prepare the [**DMP5** ⊃ **DIB**] inclusion complex, **DMP5** (10 mg dissolved in DCM/1,4-diiodobutane solution (9 : 1; v/v, 1 mL) was subjected to solvent diffusion with methanol (5 mL).

ITC measurements

For the ITC host–guest complexation experiments, **DMP5** dissolved in $CHCl_3$ (300 μL, 10 mM) was added to the reaction cell,

while $CHCl_3$ was placed in the reference cell. The 1,4-dihalobutane guests were prepared at a concentration of 100 mM. The titration was carried out with 32 injections of 2 μL each, with a time interval of 240 s between injections. In the ITC dilution experiments, a 10 mM solution of the self-assembled inclusion complexes [**DMP5** ⊃ **BXB**] system in $CHCl_3$ was loaded into a syringe and automatically titrated with 2 μL per injection, at a time interval of 240 s, into a reaction cell containing pure $CHCl_3$ (300 μL). The dissociation of the self-assembled aggregates was observed through non-constant heat signals, accompanied by a constant heat of dilution. A control experiment was conducted using a 10 mM **DMP5** chloroform solution without the guest molecule, under conditions similar to those used for the inclusion complex, against pure $CHCl_3$. All titrations were performed at 298 K.

Conclusion

In conclusion, a self-assembled supramolecular polymer based on a permethylated pillar[5]arene (**DMP5**) mediated by guest halogen–halogen interactions was developed. Host–guest complexation studies between **DMP5** and 1,4-difluorobutane (**DFB**), 1,4-dichlorobutane (**DCB**), 1,4-dibromobutane (**DBB**), and 1,4-iodobutane (**DIB**) revealed that the type of halogen in the guest molecule significantly influences the complexation behavior. Our findings from ^{1}H NMR titration and ITC measurements consistently demonstrated the formation of a 1 : 1 inclusion complex in solution, corroborating well with the solid-state single-crystal X-ray analysis. Furthermore, our investigation into the inclusion complexes [**DMP5** ⊃ **DCB**], [**DMP5** ⊃ **DBB**], and [**DMP5** ⊃ **DIB**] revealed their ability to promote the formation of supramolecular polymers *via* halogen–halogen guest interactions. This was confirmed by single-crystal X-ray analysis, ^{1}H diffusion studies, and ITC dilution experiments. Notably, utilizing ITC dilution experiments, provided insights into the enthalpically favorable nature of self-assembly, which was found to be influenced by the nature of halogen–halogen interactions. Dissociation constant and diffusion measurements demonstrated that [**DMP5** ⊃ **DIB**] formed the most stable supramolecular polymer assembly. In contrast, the inclusion complex of [**DMP5** ⊃ **DFB**] exhibited behavior similar to ITC dilution experiments conducted with **DMP5** in the absence of a guest molecule, indicating that fluorine did not contribute significantly to the formation of supramolecular assemblies *via* halogen–halogen interactions. Moreover, the disassembly of the supramolecular polymer promoted by 4-dimethylaminopyridine (**DMAP**) was studied for [**DMP5** ⊃ **DIB**] by ^{1}H NMR and ITC. ITC dilution experiments revealed that supramolecular polymer dissociation is enthalpically and entropically driven. ^{1}H NMR analysis further revealed shows the formation of N···I bonding interactions at both ends of the inclusion guest. Further studies on the supramolecular self-assemblies of various pillar[5]arenes and guest compounds are underway in our laboratory, aiming to deepen our understanding of their complexation behavior and potential applications.

Data availability

The data supporting this article have been included as part of the ESI.†

Conflicts of interest

There are no conflicts to declare.

Acknowledgements

The support received from Kuwait University was made available through Research Grant No. SC08/19 and the facilities of the RSPU (Grant No. GS01/01, GS03/01, GS01/03, GS01/10, and GS03/08) are gratefully acknowledged.

References

1 (*a*) V. Amendola, D. Esteban-Gomez, L. Fabbrizzi and M. Licchelli, *Acc. Chem. Res.*, 2006, **39**, 343–353; (*b*) D. J. Lundberg, C. M. Brown, E. O. Bobylev, N. J. Oldenhuis, Y. S. Alfaraj, J. Zhao, I. Kevlishvili, H. J. Kulik and J. A. Johnson, *Nat. Commun.*, 2024, **15**, 3951.
2 P. D. Beer and P. Schmitt, *Curr. Opin. Chem. Biol.*, 1997, **1**, 475–482.
3 (*a*) P. D. Beer and P. A. Gale, *Angew. Chem., Int. Ed.*, 2001, **40**, 486–516; (*b*) K. Buaksuntear, P. Limarun, S. Suethao and W. Smitthipong, *Int. J. Mol. Sci.*, 2022, **23**, 6902; (*c*) S. Talreja and S. Tiwari, *Int. J. Pharm. Phytopharm. Res.*, 2023, **7**, 133–139.
4 V. Bojinov and N. Georgiev, *J. Univ. Chem. Technol. Metall.*, 2011, **46**, 3–26.
5 C. R. Bondy and S. J. Loeb, *Coord. Chem. Rev.*, 2003, **240**, 77–99.
6 N. Busschaert, I. L. Kirby, S. Young, S. J. Coles, P. N. Horton, M. E. Light and P. A. Gale, *Angew. Chem., Int. Ed.*, 2012, **51**, 4426–4430.
7 N. Busschaert and P. A. Gale, *Angew. Chem., Int. Ed.*, 2013, **52**, 1374–1382.
8 R. H. Crabtree, K. Kavallieratos and C. M. Bertao, *J. Org. Chem.*, 1999, **64**, 1675–1683.
9 P. A. Gale, *Acc. Chem. Res.*, 2006, **39**, 465–475.
10 P. A. Gale, *Chem. Commun.*, 2011, **47**, 82–86.
11 R. Martinez-Manez and F. Sancenon, *Chem. Rev.*, 2003, **103**, 4419–4476.
12 C. H. Park and H. E. Simmons, *J. Am. Chem. Soc.*, 1968, **90**, 2431–2432.
13 R. Pomecko, Z. Asfari, V. Hubscher-Bruder, F. Arnaud-Neu and M. Bochenska, *Supramol. Chem.*, 2010, **22**, 275–288.
14 J. W. Steed and J. L. Atwood, *Supramol. Chem.*, John Wiley & Sons Ltd, 2009.
15 E. Wagner-Wysiecka and J. Chojnacki, *Supramol. Chem.*, 2012, **24**, 684–695.
16 C. R. Yamnitz, S. Negin, I. A. Carasel, R. K. Winterb and G. W. Gokel, *Chem. Commun.*, 2010, **46**, 2838–2840.
17 J.-M. Lehn, *Supramolecular Chemistry: Concepts and Perspectives*, VCH, Weinheim, 1995.

18 J. W. Steed and J. L. Atwood, *Supramolecular Chemistry: an Introduction*, Wiley, Chichester, 2000.
19 T. Ogoshi, T.-A. Yamagishi and Y. Nakamoto, *Chem. Rev.*, 2016, **116**, 7937–8002.
20 T. Ogoshi, T. Kakuta and T.-A. Yamagishi, *Angew. Chem., Int. Ed.*, 2018, **58**, 2197–2206.
21 M. Xue, Y. Yang, X. Chi, Z. Zhang and F. Huang, Pillararenes, *Acc. Chem. Res.*, 2012, **45**, 1294–1308.
22 N. L. Strutt, H. Zhang, S. T. Schneebeli and J. F. Stoddart, *Acc. Chem. Res.*, 2014, **47**, 2631–2642.
23 T. Kakuta, T.-A. Yamagishi and T. Ogoshi, *Acc. Chem. Res.*, 2018, **51**, 1656–1666.
24 T. Xiao, W. Zhong, L. Xu, X.-Q. Sun, X.-Y. Hu and L. Wang, *Org. Biomol. Chem.*, 2019, **17**, 1336–1350.
25 K. E. Krakowiak, J. S. Bradshaw and D. J. Zamecka-Krakowiak, *Chem. Rev.*, 1989, **89**, 929–972.
26 J. S. Bradshaw and R. M. Izatt, *Acc. Chem. Res.*, 1997, **30**, 338–345.
27 G. W. Gokel, W. M. Leevy and M. E. Weber, *Chem. Rev.*, 2004, **104**, 2723–2750.
28 A. Harada, A. Hashidzume, H. Yamaguchi and Y. Takashima, *Chem. Rev.*, 2009, **109**, 5974–6023.
29 A. C. Bhasikuttan, H. Pal and J. Mohanty, *Chem. Commun.*, 2011, **47**, 9959–9971.
30 Z. Asfari, V. Boehmer, J. Harrowfield, J. Vicens and M. Saadioui, *Calixarenes*, Springer Netherlands, 2001.
31 C. D. Gutsche, *Calixarenes, an Introduction*, The Royal Society of Chemistry, Cambridge, U.K., 2nd edn, 2008.
32 E. Botana, E. Da Silva, J. Benet-Buchholz, P. Ballester and J. de Mendoza, *Angew. Chem., Int. Ed.*, 2007, **46**, 198–201.
33 (*a*) N. Morohashi, F. Narumi, N. Iki, T. Hattori and S. Miyano, *Chem. Rev.*, 2006, **106**, 5291–5316; (*b*) Z. Zhang, B. Xia, C. Han, Y. Yu and F. Huang, *Org. Lett.*, 2010, **12**(15), 3285–3287; (*c*) Z. Zhang, Y. Luo, J. Chen, S. Dong, Y. Yu, Z. Ma and F. Huang, *Angew. Chem., Int. Ed.*, 2011, **50**, 1397–1401; (*d*) W. Yang, W. Zhang, J. Chen and J. Zhou, *Chin. Chem. Lett.*, 2024, **35**, 108712.
34 W. Maes and W. Dehaen, *Chem. Soc. Rev.*, 2008, **37**, 2393–2402.
35 M.-X. Wang, *Acc. Chem. Res.*, 2012, **45**, 182–195.
36 X. Li, Y. Jin, N. Zhu and L. Y. Jin, *Polymers*, 2023, **15**, 4543.
37 P. Liu, Z. Li, B. Shi, J. Liu, H. Zhu and F. Huang, *Chem.–Eur. J.*, 2018, **24**, 4264–4267.
38 K. Eichstaedt, B. Wicher, M. Gdaniec and T. Połoński, *CrystEngComm*, 2016, **18**, 5807–5810.
39 L. C. Gilday, S. W. Robinson, T. A. Barendt, M. J. Langton, B. R. Mullaney and P. D. Beer, *Chem. Rev.*, 2015, **115**, 7118–7195.
40 A. Priimagi, G. Cavallo, P. Metrangolo and G. Resnati, *Acc. Chem. Res.*, 2013, **46**, 2686–2695.
41 P. Metrangolo, F. Meyer, T. Pilati, G. Resnati and G. Terraneo, *Angew. Chem., Int. Ed.*, 2008, **47**, 6114–6127.
42 S. Välimäki, L. Gustavsson, N. K. Beyeh, V. Linko and M. A. Kostiainen, *Macromol. Rapid Commun.*, 2019, **40**, 1900158.
43 (*a*) G. Cavallo, P. Metrangolo, R. Milani, T. Pilati, A. Priimagi, G. Resnati and G. Terraneo, *Chem. Rev.*, 2016, **116**, 2478–2601; (*b*) B. K. Saha, R. V. P. Veluthaparambath and V. Krishna G, *Chem.–Asian J.*, 2023, **18**, e202300067.
44 T. T. T. Bui, S. Dahaoui, C. Lecomte, G. R. Desiraju and E. Espinosa, *Angew. Chem., Int. Ed.*, 2009, **48**, 3838–3841.
45 A. Mukherjee, S. Tothadi and G. R. Desiraju, *Acc. Chem. Res.*, 2014, **47**, 2514–2524.
46 T. F. Al-Azemi and M. Vinodh, *Polym. Chem.*, 2020, **11**, 3305–3312.
47 N. O. Abdeljaber, M. Vinodh and T. F. Al-Azemi, *Tetrahedron*, 2023, **132**, 133240.
48 X. Shu, J. Fan, J. Li, X. Wang, W. Chen, X. Jia and C. Li, *Org. Biomol. Chem.*, 2012, **10**, 3393–3397.
49 L. Liu, W. Duan, Y. Kou, L. Wang, H. Meier and D. Cao, *Chin. J. Chem.*, 2015, **33**, 346–350.
50 M. A. Spackman and D. Jayatilaka, *CrystEngComm*, 2009, **11**, 19–32.
51 J. J. McKinnon, M. A. Spackman and A. S. Mitchell, *Acta Crystallogr., Sect. B: Struct. Sci.*, 2004, **60**, 627–668.
52 J. J. McKinnon, D. Jayatilaka and M. A. Spackman, *Chem. Commun.*, 2007, **37**, 3814–3816.
53 M. J. Turner, J. J. McKinnon, S. K. Wolff, D. J. Grimwood, P. R. Spackman, D. Jayatilaka and A. M. Spackman, *CrystalExplorer17*, University of Western Australia, 2017, **http://hirshfeldsurface.net**.
54 B. K. Saha, R. V. P. Veluthaparambath and V. Krishna, *Chem.–Asian J.*, 2023, **18**, e202300067.
55 M. Capdevila-Cortada and J. J. Novoa, *CrystEngComm*, 2015, **17**, 3354–3365.
56 K. E. Riley and K.-A. Tran, *Faraday Discuss.*, 2017, **203**, 47–60.
57 T. Ogoshi, T. Aoki, K. Kitajima, S. Fujinami, T. A. Yamagishi and Y. Nakamoto, *J. Org. Chem.*, 2011, **76**, 328–331.
58 P. Thordarson, *Chem. Soc. Rev.*, 2011, **40**, 1305–1323.